Journal of Computational Methods in Sciences and Engineering -1 (2016) 1–15 1
DOI 10.3233/JCM-160659
IOS Press

Exploring the effect of the *O*-(1-heptylnonyl) benzene sulfonate surfactant on the nature of the linear hydrocarbons/water interface by means of an atomistic molecular dynamics simulation

Yosslen Aray[a,b,d,*], José Gregorio Parra[c], Doris Marianela Jiménez[a], Ricardo Paredes[e], Alejandro Martiz[d], Samantha Samaniego[f], Mauricio Cornejo[d], Eduardo V. Ludena[a,d] and Cecilia Paredes[d]

[a]*Laboratorio de Fisicoquímica Teórica de Materiales, Centro de Química, Instituto Venezolano de Investigaciones Científicas, IVIC, Caracas, Venezuela*
[b]*Facultad de Ciencias, Universidad de Ciencias Aplicadas y Ambientales, UDCA, Campus Universitario Norte, Bogotá, Colombia*
[c]*Laboratorio de Química Computacional, Dpto. de Química, Facultad Experimental de Ciencias y Tecnología, Universidad de Carabobo, Edo. Carabobo, Venezuela*
[d]*Facultad de Ingeniería Mecánica y Ciencias de la Producción, Escuela Superior Politécnica del Litoral, ESPOL, Guayaquil, Ecuador*
[e]*Facultad de Ingeniería en Ciencias de la Tierra, ESPOL, Campus Gustavo Galindo, Guayaquil, Ecuador*
[f]*Departamento de Física, Facultad de Ciencias Naturales y Matemática, ESPOL, Campus Gustavo Galindo, Guayaquil, Ecuador*

Abstract. Using molecular dynamics simulations a systematic study of the binding energy per cross sectional area for the water/n-alkane (hexane, octane, decane, dodecane and tetradecane) interfaces was performed. The effect of the Sodium p-(1-heptylnonyl) benzene sulfonate surfactant, on the adhesion forces of the water/n-hydrocarbon (decane, undecane, dodecane, and tetradecane) interfaces was studied. Scanning of the binding energy per area against n-alkanes shows that the magnitude of this parameter for the surfactant tail-alkane interactions at the interface systematically increases with the chain length of the alkane, whereas it shows a maximum at undecane for the water-surfactant head interactions at the interface. This maximum of head adhesion forces thus agrees with the reported minimum value of the interfacial tension at undecane for the p-(1-heptylnonyl) benzene sulfonate, suggests that for the water/alkane interface it is this trend in surfactant head adhesion at the interface that defines that interfacial tension minimum value.

Keywords: Linear alkyl benzene sulfonates, molecular dynamics, hydrocarbon water interface, binding energies per area

*Corresponding author: Yosslen Aray, Facultad de Ciencias, Universidad de Ciencias Aplicadas y Ambientales, UDCA, Campus Universitario Norte, Calle 222 No 55-37, Bogotá, Colombia. Tel.: +571 6684700; E-mail: yaray@udca.edu.co.

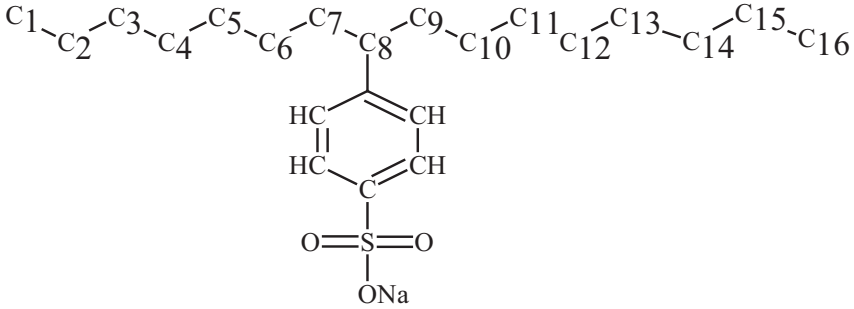

Fig. 1. Chemical structure of the 8-C16 surfactant.

1. Introduction

The interfacial properties of the adsorption film formed by surfactant molecules at oil/water interface play a crucial role on many scientific technological processes such as oil recovery [1–3]. In order to obtain the maximum benefit from surfactants used in this process a good knowledge of their interface behavior is demanded [3]. Additionally, in designing new types of the most efficient oil-displacing surfactants, the key question is how to gain an insight into the structure/function relationship of these materials [1]. In this sense, many studies have been reported from both experimental [1–16] and theoretical points of view [17–24]. A considerable number of experimental research works have been reported concerning interface properties such as the behavior of interfacial tension (*IFT*), area per surfactant molecule (A), density profile, etc., between oil and water for alkyl benzene sulfonates [2–4,8,11], alkyl methylnaphthalene sulfonates [9], Gemini surfactants [7], other quite complicated surfactant system such as sorbitan [5] and also at the air water interface [12–16]. Molecular dynamics simulation of similar properties, namely, surface tensions, density profiles and several radial distribution functions of surfactant monolayers at the air/water [17–22] and hydrocarbons/water [23,24] interfaces, have also been reported. Molecular simulations have become an important tool for the study of the complex interface systems, as they are capable of providing quite accurate estimates of the dynamical, thermodynamical and structural properties of the interface system at the molecular level [24].

Sodium linear alkylbenzene sulfonates (LAS) belong to the kind of very popular surfactants which are widely used in industry and daily life. In fact, linear alkyl benzene sulfonates form the most important synthetic surfactant family in the world [20]. This compound has a sulfonate group and a linear alkyl chain which is usually attached to the *para* positions of a benzene ring (Fig. 1). The alkyl chain may have $m + n$ carbons atoms with the benzene ring attached to the $(m + 1)$ carbon $(m < n)$ [20]. The specific example in Fig. 1 has a chain of 16 carbons atoms, and the benzene ring is attached to the 8th carbon. This is the O-(1-hetylnonyl) benzene sulfonate, more briefly denoted as 8-phenyl hexadecane sulfonate, 8-C16. These surfactants may be regarded as *Cn* alkyl benzene sulfonates with a substituted *Cm* alkyl chain. Previous works [4,24] have clearly indicated that the nearer to the end of the chain the benzene ring is attached, the lower the molecular weight is of the alkane which yields the lowest *IFT*. In general, when the total number of carbons atoms in the alkyl chain of the surfactant is increased, the minimum in *IFT* appears at a higher alkane carbon number [4]. Scanning of interfacial tensions against all or part of the homologous series of n-alkanes is a useful method [4,8,11] of characterizing the low tension behavior of surfactants and oil at the water/oil interface. Each surfactant shows a minimum tension at a particular n-alkane carbon number. In this way, a key concept is the alkane carbon number, n_{min},

corresponding to the minimum *IFT* when measured against an n-alkane series. For the 8-C16 case the optimum n_{min} at undecane was experimentally determined [4].

Deep insights into the nature of the interaction at the molecular level between the immiscible phases and the surfactant at the interface can be gained by studying the adhesive forces operating at that interface. In the present paper, to get a better understanding of the behavior of surfactants, we have performed a systematic study of those forces calculated as the interaction energy or binding energy per area for the water/n-alkane (hexane, octane, decane, dodecane and tetradecane) interface, for the 8-C16 monolayer at the water/vacuum interface and for this monolayer at the n-alkane (decane, undecane, dodecane and tetradecane)/water interface. As a result, through the use of the concept of adhesive forces we have been able to explain in greater detail the origin of the minimum of the *IFT* for 8-C16 at C11 and have gained a more adequate understanding of the nature of the interface interactions.

2. Methods

2.1. Adhesion and interfacial tension.

The work of adhesion, W_{12}, is the free energy change, or reversible work per unit area done to separate to infinity two different media initially in contact, a process that results in the creation of two new surfaces [25]. W_{ij} it is related to the intermolecular forces that operate at the interface between the two media. When the media are liquids W_{ij} is defined by the equation of Dupre as [25],

$$W_{ij} = \gamma_i + \gamma_j - \gamma_{ij} \tag{1}$$

Where γ_i and γ_j are the surface tensions of the two individual liquids and γ_{ij} is the *IFT* between the two liquids in contact. For two identical media, the work of cohesion, W_i for the liquid i is given by

$$W_i = 2\gamma_i \tag{2}$$

From Eqs (1) and (2), the relationship between the work of adhesion and *IFT* can be written as,

$$\gamma_{ij} = \frac{1}{2}(W_i + W_j) - W_{ij} \tag{3}$$

This equation suggests that the interfacial tension results from the competition between the cohesion forces holding molecules together in the separate liquids and the adhesive forces at the interface [25]. Experimental reports [26–28] of measured *IFT* for the n-hydrocarbon water interface, hyd/wat, with the n-hydrocarbon going from C_6 to C_{16}, have clearly shown that there is a linear relationship with the number of carbon, n_{Ci}, of the chain length: *IFT* systematically increases as n_{Ci} increases.

Equation (3) has very important implications for enhanced oil recovery (EOR). In EOR, surfactant formulations are injected into the reservoirs to reduce the interfacial tension to very low values between the aqueous chemical solution and the crude oil, with the purpose of mobilizing the oil and thus producing more oil than by conventional methods. Equation (3) shows that by increasing W_{ij} it is possible to obtain very low values of $\gamma_{Hyd/Wat}$. This is just the role [29] of the surfactant: to produce an appreciable increase of the adhesive forces between the interfaces involved in the water/surfactant/oil systems.

The energy change for separating two media i and j in a medium k [29], such as a surfactant monolayer (medium k) between hydrocarbon/water interfaces is given sby

$$W_{ikj} = (W_k + W_{ij}) - (W_{ik} + W_{jk}) \tag{4}$$

Where W_k is the work of cohesion between the surfactant molecules, while W_{ij} is the corresponding work of adhesion water/hydrocarbon. In the case when the surfactant forms an entire monolayer, W_{ij} will be negligible (there is no direct contact water-hydrocarbon) and adhesion only involves forces between the surfactant and the water and hydrocarbon phases.

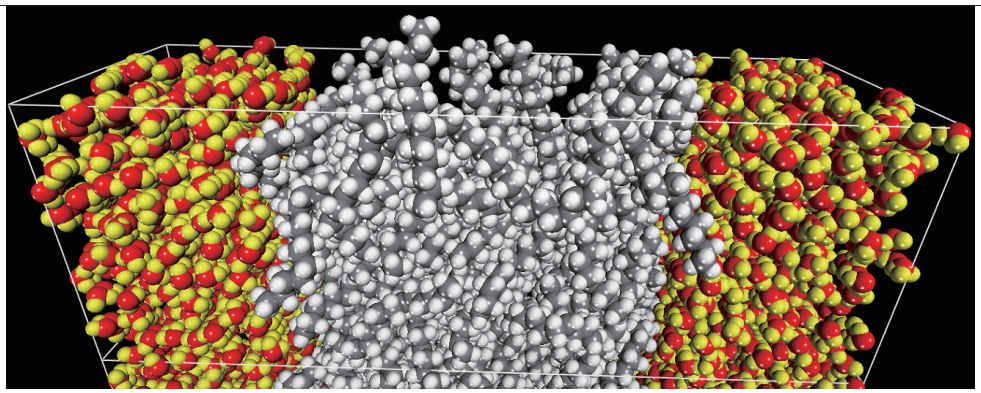

(a)

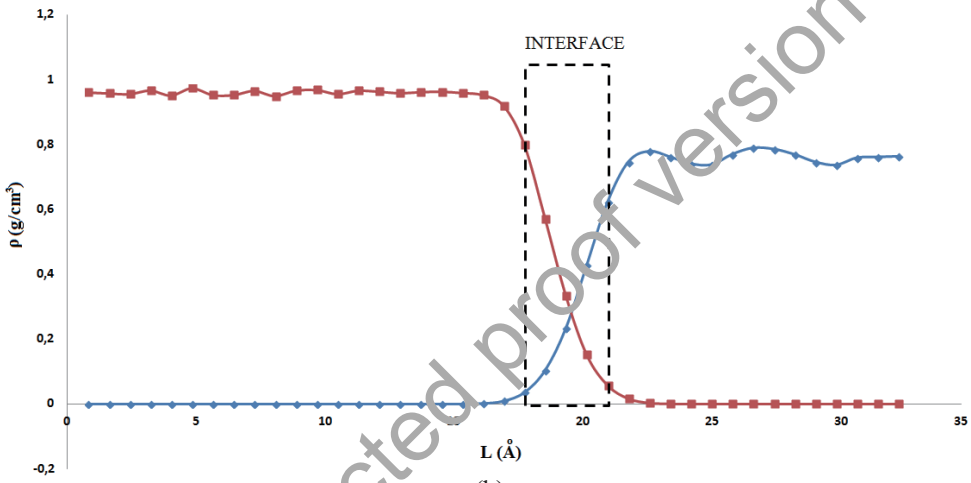

(b)

Fig. 2. (a) Simulation box of the water/n-hydrocarbon interfaces. Red and yellow spheres denote the oxygen and hydrogen atoms of the water molecules while gray and white spheres denote the carbon and hydrogen atoms of the Cn molecules. (b) Density profile along the z-axis normal to the interface at the left for the water molecules (red line) and C14 molecules (blue line). The perpendicular axis corresponds to the density in gr/cm^3 and the horizontal one to the position (Å) along the z-axis. Heavy black lines define the interface zone.

2.2. Calculations

The hydrocarbons/water interface was determined by running a combination of NVT (constant volume and temperature) and NPT (constant pressure and temperature) molecular dynamics simulations for a cell under periodic boundary conditions [22]. An orthorhombic simulation box with dimension of 34 Å $\times$ 34 Å $\times$ 110 Å containing two water-hydrocarbon interfaces (Fig. 2a) with 900 water molecules and 1080/n_{Ci} hydrocarbon molecules (1080 carbon atoms per molecule) was initially constructed. These simulation boxes have similar dimensions as those used in previous molecular dynamic studies of the water/n-alkane interface [24]. First the hydrocarbon and water phases were prepared separately using the Amorphous Builder software [30] to create an initial random and low density sample using a suitable Monte Carlo procedure to achieve a right distribution of conformational states. After that, the two phases were integrated into the simulation box. The next step was an energy minimization to relax the system. Finally, NVT and NPT simulations were sequentially carried out to equilibrate the system. First, a NVT

Table 1
Equilibrated Cell parameters of the orthorhombic simulation box, calculated density and interfacial thickness, *IT*, of the hydrocarbon/water system

n_{Ci}	a	b	c	Calculated density (g/cm^3)	Hydrocarbon Experimental density [33]	IT calc Å	IT Exp [34]	IT Estimated [34]
6	25.545	25.545	75.132	0.754 ± 0.006	0.659	3.76	3.5 ± 0.2	3.99
8	25.242	25.242	74.240	0.780 ± 0.006	0.703	4.02	5.5 ± 0.2	4.28
10	25.000	25.000	73.529	0.802 ± 0.0062	0.730	4.41	4.6 ± 0.2	4.58
12	26.045	26.045	76.603	0.804 ± 0.0056	0.749	4.60	5.0 ± 0.2	4.89
14	27.384	27.384	80.540	0.839 ± 0.0056	0.763	4.83		5.20

simulation was performed for 4 ns at 300K to thermalize and equilibrate the system. Then, a NPT simulation for 4ns at 300K was done to adjust the system to the right density. To obtain a good statistic at constant volume, a final equilibration was performed by means of a NVT simulation for 4ns. Forcite software [31] with Compass force field [32] for the MD simulations was used.

Forcite [31] allows the possibility to extract potential energy contribution between pre-specified groups defined as sets. The work of adhesion, taken as the binding energy (BE $= \mathrm{E}_{AB} - (\mathrm{E}_A + \mathrm{E}_B)$) per cross sectional area for each pair of sets can be calculated along the trajectory, taking a final averaging of the calculated values. A script in Perl program language was written for that purpose.

3. Results and discussion

3.1. Water/n-alkanes interfaces

The cell parameters of the simulation box resulting from the equilibration process are collected in Table 1. The obtained density in g/cm^3 is also summarized in Table 1. Density fluctuations less than 1% of the average values for subsequent NPT steps were observed. Note that the density of the total system shows an intermediate value between that of the pure bulk phase, 0.997 g/cm^3 for water and those of the linear hydrocarbons [33] (also reported in Table 1). The present result for C10 is in good agreement with the value calculated in ref. [23] (0.81$\pm$ 0.01 g/cm^3). In general, the density of the hydrocarbon/water system increases with the density of the hydrocarbons and shows a systematic increase with the hydrocarbon chain length. Density profiles of each system along the Z-axis direction of the simulation box were also calculated by dividing the system into $Z/100$ thick slabs parallel to the *xy* plane. Figure 2(b) shows the density profile for water/C14 box. Two well-defined interfaces can be observed. The alkane densities show significant fluctuations with peaks of about 5A from one another. In a previous report [24] a similar effect was observed and it has suggested that these peaks correspond to the position of minimum energy for the carbon Lennard-Jones potential. This means that alkane density fluctuations do not dissipate until far from the alkane/water interface and that small potential system size effects may be present in the alkane phase.

The interfacial thickness, *IT*, between the hydrocarbons and water phases was determined using the "90-90" criteria which is the distance between two positions where the densities of hydrocarbon and water are 90% of their own bulk densities [23]. The calculated *IT* values are in good agreement with the measured thickness (see Table 1) observed from the synchrotron X-ray reflectivity experiment [34], except for octane where an anomalous experimental high value was reported. Additionally, in that work, an estimation combining the capillary-wave prediction, σ^2_{cap}, with a contribution from the intrinsic structure was reported. The intrinsic contribution was chosen to be the radius of gyration, *Rg*, of the alkane. These

Table 2
Calculated n-alkane/water work of adhesion

n_{Ci}	BE/area (dyn/cm)	Wij exp (dyn/cm) [26]
6	43.693	40.9
8	45.370	43.3
10	46.850	44.9
12	47.905	45.8
14	49.104	46.6

estimated values are shown in the last column of Table 1. It can be seen that our calculated *IT* values show the same trend as the estimated *IT* values and a good linear relationship $IT_{calc} = 1.098\ IT_{estimat}$ – 0.158 with $R^2 = 0.98$ was found. Note also that the interfacial thickness grows monotonically with the length of the n-alkane chain. i.e., it increases with the number of carbon atoms. The following linear relation with the carbon number, $IT_{calc} = 0.136\ n_{Ci} + 2.964$; $R^2 = 0.99$ was determined. Thus the present results corroborate the linear variation of the interfacial width for the water/n-alkane interface with the alkane length chain.

Finally, to estimate the work of adhesion at the interface we have calculated the binding energy per cross sectional area, *BE/area*, and the results are collected in Table 2. The experimental values for the work of adhesion for the studied interfaces are shown, as well, in this Table. The agreement with the experiment is good and validates our adhesion calculations. The calculated *BE/area* values indicate that the adhesion at the interface shows the same behavior as that evinced by the density and *IT* with respect to the hydrocarbon chain length, namely, a linear increase of *BE/area* with n_{Ci}: *BE/area* $= 0.706\ n_{Ci} + 43.080$; $R^2 = 0.97$.

BE/area is a measurement of the adhesive forces between the water and hydrocarbon molecules at the interface and depends on the intrinsic structure of this interface. Experimental measurements of the nonlinear susceptibility using optical second harmonic generation [35] have suggested the presence of highly ordered n-alkanes molecules at the interface; similarly, molecular simulation studies [36] have shown a preferred parallel orientation of the n-alkanes molecules close to the interface. We have checked our simulation boxes for the studied interfaces and for all these cases we have corroborated the favored parallel orientation of the hydrocarbon molecules at the interface. For example, Fig. 3 shows the snapshot (4000 ps of the last simulation step) at the interface (depth Δ Z= 4.83 Å) for the water/C14 cases where the H atoms were deleted. Red spheres denote the water oxygen atoms and the yellow ones the C14 molecules inside the interface in parallel orientation (see Fig. 3a); the blue and green molecules only have their end parts inside the interface. Thus, the present results support the parallel orientation of the studied n-alkane molecules at the water/alkane interface. This orientation will produce the best packing of the molecules favored by the H_2O-CH_2 interaction. At the interface the structures of both water and n-alkane are different from those in the bulk: there occurs a decrease in the density of the water molecules at the interface due to a local expansion of the structure of these molecules (this can be seen in Fig. 2), whereas there is an increase in the local density of alkanes due to their local concentration at the interface (see Table 1 and Fig. 2). The alkane molecules are laterally oriented with respect to the interface in order to be in close contact with water. Hence, because the alkane molecules lay somewhat flat against the water surface in order to maximize surface contact they minimize penetration into the water phase. The combination of the water expansion and a more marked inclination of the alkane molecules as the chain gets larger could be at the origin of the IT increase. The increase in the alkane density should produce an increase in the number of water molecules having their hydrogens pointing towards the carbons of the alkane phase and thus showing greater orientation preference. All these factors contribute toward increasing the number of water molecules having greater contact with the alkane molecules, which, in

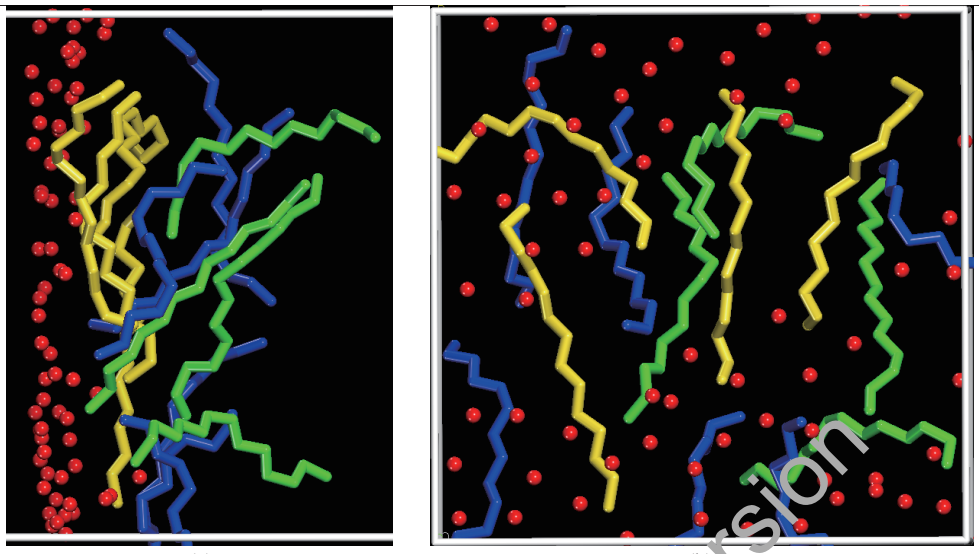

(a) (b)

Fig. 3. Snapshot of the C14 molecules at the water/C14 interface. (a) Interface side view and (b) top-view (perpendicular to the z-axis). For visual clarity the hydrogen atoms have been removed. Red spheres denote the water oxygen atoms while yellow sticks denote the C14 molecules closets to the interface. Note in (a) that the yellow molecules are parallel to the interface.

turn produce an adhesion increase at the interface. However, additional studies about the inclination degree of the alkane molecules at the interface as then chain length increases should be done.

At this point, we would like to emphasize that the above results suggest that the COMPASS force field provides an acceptable accuracy for describing the interfacial n-hydrocarbon/water system in which we are interested.

3.2. 8-C16 monolayers at the air/water interface

At the air/water interface, water molecules are subjected to unequal short-range attraction forces and produce a net inward pull into the bulk phase [29]. Minimization of the contact area with the gas phase is therefore a spontaneous process. Depending on the surfactant molecular structure, adsorption takes place over various concentration ranges and rates. Above a well-defined concentration (the critical micelle concentration – CMC) micellization or aggregation takes place. At the CMC, the interface is at its maximum coverage forming an adsorbed surfactant monolayer. Above the CMC value, molecules begin to aggregate in the bulk phase [29]. Understanding the structure and properties of the adsorbed monolayer is of considerable interest not only because of their scientific significance but also because of their importance in a number of industrial and technological processes. In order to obtain information about the microscopic nature of the monolayer of amphiphilic molecules at the water/air interface, different experimental techniques including fluorescence, resonance Raman scattering, neutron reflection, second harmonic generation, Brewster angle microscopy, atomic force microscopy, calorimetry, X-ray, etc, have been performed [15,19]. Special attention has been given to the study of the monolayer structure, its dynamic properties (extension of the chains, thickness of the monolayer, etc.) [19,39,40] and its interfacial properties (surface excess concentration at surface saturation, *minimal* area per molecule at the air-water interface, $\mathcal{A}$, and standard free energy of adsorption, ΔG^0_{ad}, etc.). Information related to the degree of packing and the orientation of the adsorbed surfactant molecules at the interface is provided by the area

Table 3
Reported experimental $\mathcal{A}$ values for head group positional isomers of sodium para-dodecyl benzene sulfonate and sodium hexadecyl o-xylene sulfonates

	Structure	$\mathcal{A}$ (Å^2) at 25°C
2-C_{12}BS [41]	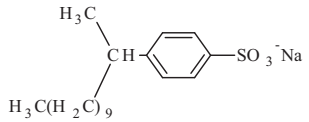	43
3-C_{12}BS [41]	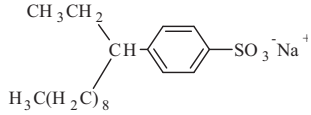	54
4-C_{12}BS [41]	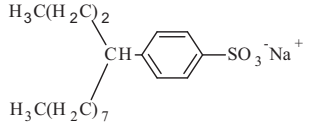	55
5-C_{12}BS [41]	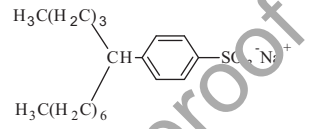	61
6-C_{12}BS [41]	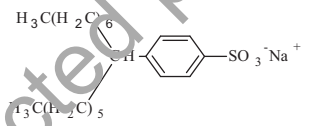	65
3-C16*o*-XS [14]	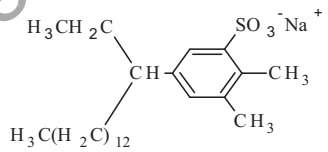	47.38
5-C16*o*-XS [14]	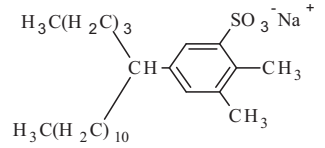	79.67
7-C16*o*-XS [14]	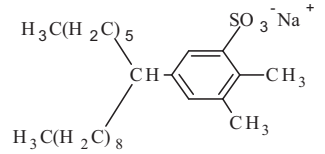	88.83

Table 4
Calculated average values of the area per molecule, $\mathcal{A}$, interfacial thickness and binding energy per interfacial area for 6 to 12 surfactant molecules at the 8-C16/water interface

	A (Å^2)	Interfacial thickness Å	-*BE/area* (Wat/8-C16) (dyn/cm)
6	96.000	6.50	1088.716
7	82.29	6.63	1382.831
8	72.000	6.70	1502.462
10	57.600	6.75	1062.244
12	48.000	6.80	1034.644

per molecule parameter, which is a measurement of the interface coverage density. Experimental $\mathcal{A}$ values for six monodispersed head group positional isomers (see Table 3) of sodium *para*-dodecyl benzene sulfonate (C12BS) have been recently reported (43 Å^2 to 65 Å^2) at CMC [41]; for sodium hexadecyl o-xylene sulfonate [14] the values lie between 47.38 and 88.83 Å^2 (see Table 3) . We have not found experimental values for the corresponding parameter for 8-C16.

In the present work, in order to calculate A, we have constructed simulation boxes of 24 Å $\times$ 24 Å in the x and y directions and 100 Å in the z direction (see Fig. 4) and have placed inside the box 900 water molecules to form an initial 40 Å thick slab with a density of 1.0 g/cm^3 . Then, 8-C16 molecules were placed with the hydrocarbon chains extending perpendicularly with respect to the *xy* plane in all-trans conformation, distributed averagely in that plane, and with the hydrophilic head pointing into the water and the alkyl tails pointing out to the vacuum space. Four boxes with 6, 8, 10 and 12 surfactant molecules with given area/molecules ($\mathcal{A}$) values of 96.0, 72.0, 57.6 and 48.0 Å^2, respectively, were constructed. Each system was simulated for 8 ns using an NVT ensemble; the trajectories for the last 2 ns were used for data analysis. Table 4 collects the calculated $\mathcal{A}$ values averaged along the last 2 ns of the trajectory. Simple inspection of this table shows that the larger adhesion at the interface corresponds to the 8-surfactant-molecule case (*BE/area* = 1502.462 dyn/cm). By means of a polynomial regression, the values of $\mathcal{A}$ were fitted against the *BE/area* and a minimum $\mathcal{A}$ value of 74.0 Å^2 was calculated. Unfortunately, we have not found the exact data for 8-C16 in the literature; however, our results suggest that, as one might expect, this value is larger than the corresponding one for 6-C12 (62 Å^2) [41] and smaller than that for sodium hexadecyl o-xylene sulfonates (88.83 Å^2) [14] where the benzene ring point of attachment is located at the seventh carbon of the hexadecyl tail.

Figure 4a shows a snapshot of the cross-sectional view perpendicular to the plane of the interface for the 8-molecule case, at the end of the simulation. Detailed structural properties can be obtained by studying the density profile of the components of the system along the Z direction. The different components of the surfactant molecule were computed separately each one as a set, including the carbon chain, the benzene ring group, the head group – SO_3^- and the sodium atoms. The corresponding density profiles are shown in Fig. 4b. It can be seen that the –SO_3 groups are hydrated and localized in the water phase. The benzene ring groups are also almost hydrated while the carbon chains are very nearly excluded from the interface. The degree of hydration gradually decreases along the carbon chain. Only a very small fraction of the water molecules penetrates into the hydrocarbon tails. Most of the head, the benzene ring and the sodium atoms are inside the interface.

In summary, the performed simulations for the 8-C16/water interface yield the values of $A = 74.0$ Å^2, IT = 6.7 Å and *BE/area* = 1502.462 dyn/cm. It is interesting to notice that we have found very much stronger interactions between the surfactant polar head group with sodium and water molecules than those occurring at the water/hydrocarbons interface (see Table 2). Additionally we have also found

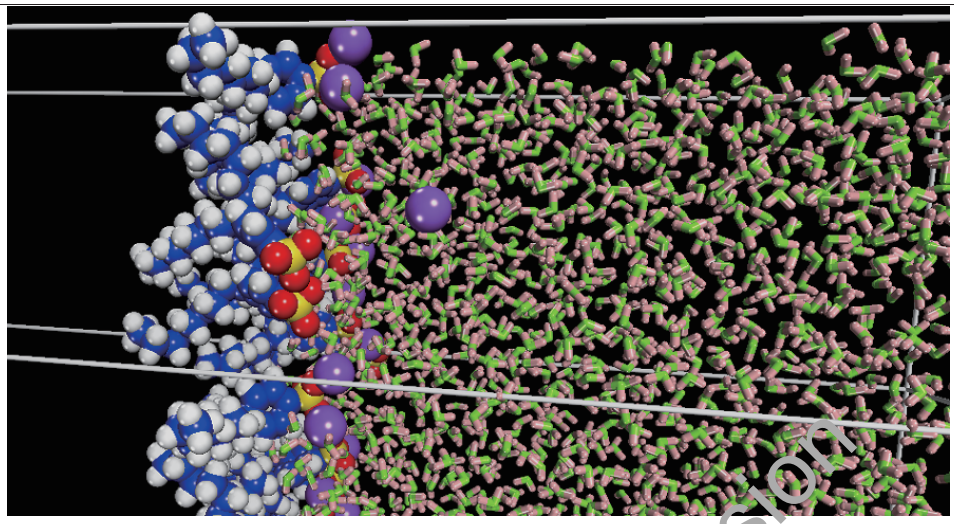

(a)

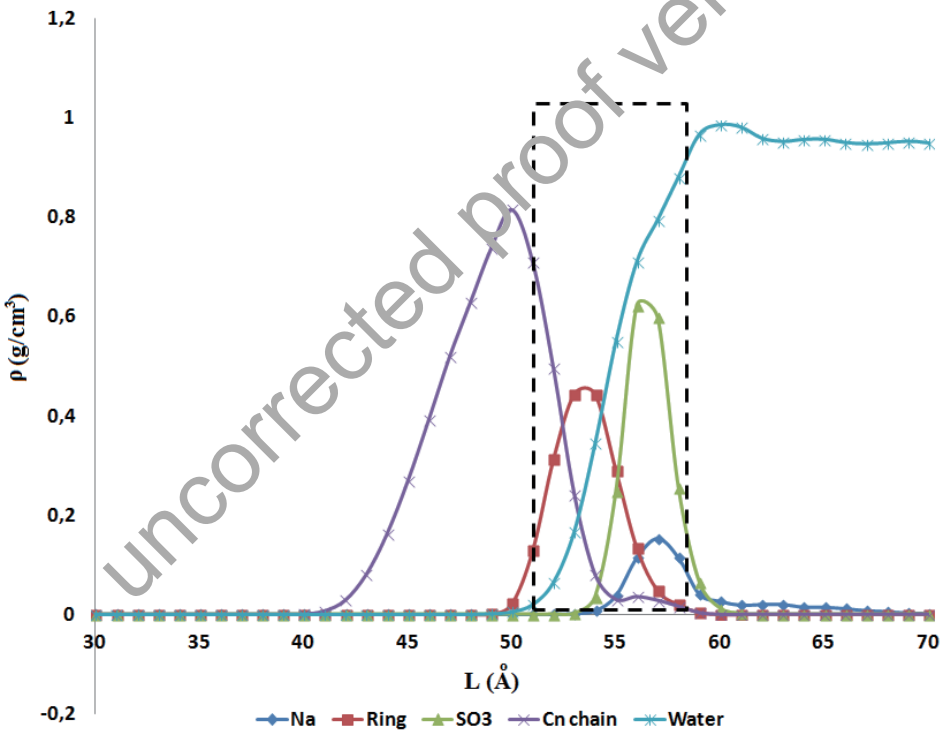

(b)

Fig. 4. (a) Interface side-view. Red, purple, yellow, blue and whites spheres denote the sodium, oxygen, sulfur, carbon and hydrogen atoms of 8-C16. Light pink and green sticks denote the hydrogen and oxygen atoms of the water molecules. (b) Density profile along the z-axis normal to the 8-C16/water interface. The sodium atoms, bencene rings, sulfonate, carbon chain and water molecules have been defined as separated sets. The perpendicular axis corresponds to the density in gr/cm^3 and the horizontal one to the position (Å) along the z-axis. Heavy broken black lines define the interface zone.

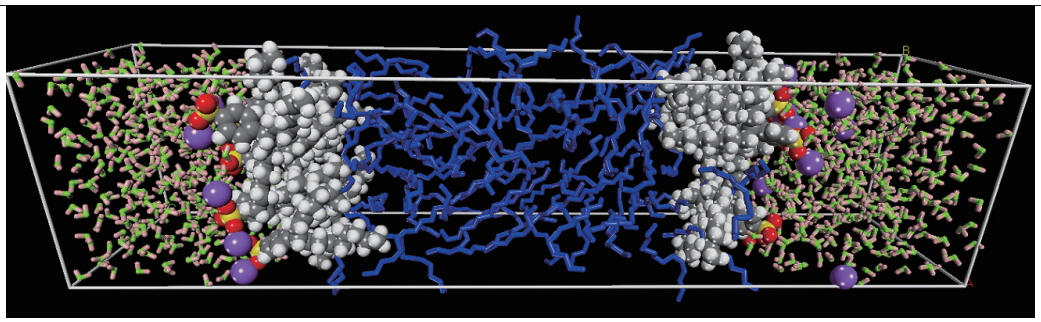

(a)

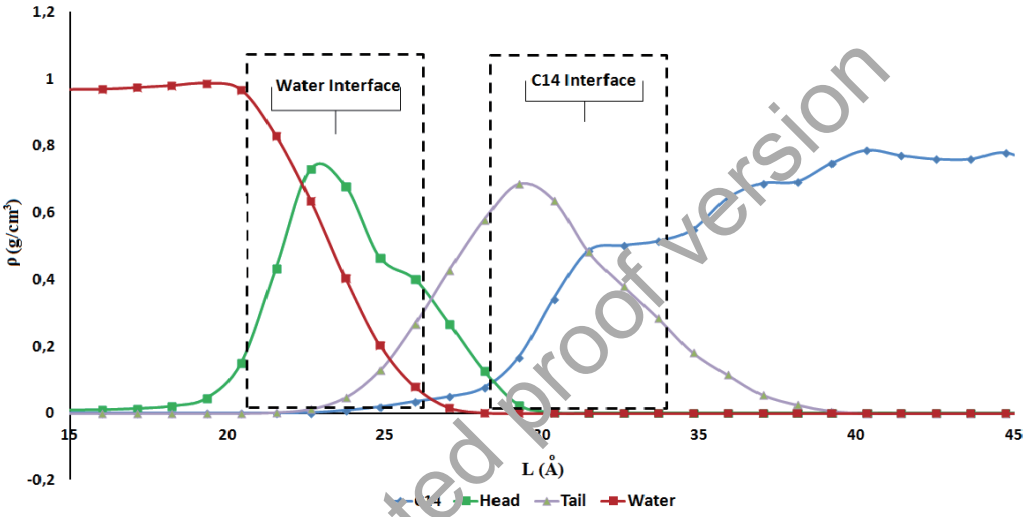

(b)

Fig. 5. (a) Simulation box of the water/8-C16/C14/8-C16/water interfaces. Red, purple, yellow, gray and whites spheres denote the oxygen, sodium, sulfur, carbon and hydrogen atoms of 8-C16. Light pink and green sticks denote the hydrogen and oxygen atoms of the water molecules. Blue sticks at the center denote the carbon atoms of C14. (b) Density profile along the z-axis normal to the interface at the left for the water molecules (red line), C14 molecules (blue line), surfactant head (green line) and surfactant hydrocarbon tail (gray line). The perpendicular axis corresponds to the density in gr/cm^3 and the horizontal one to the position (Å) along the z-axis. Heavy black lines define the interface zone.

that the surfactant head is practically hydrated and located inside the interface, whereas the carbon tails are almost entirely excluded from the water/8-C16 interface.

3.3. Influence of the 8-C16 surfactant on the nature of the C14/water interface

Simulation boxes similar to those of Fig. 2(a) with two interfaces were constructed (Fig. 5(a)). Two opposite 8-C16 monolayers at the alkane phase were built with the monolayer normal pointing in the z-direction. The monolayer/alkane/monolayer system was placed in the middle of the box. Then, the water molecules with experimental density were placed on both sides of the monolayers. The density of the alkane phase in the initial model corresponds to the experimental values. The number of water and alkane molecules was exactly the same as in the above simulations. An initial periodic box with a size of 32 Å × 32 Å × 140 Å was used and NVT and NPT MD simulations similar to those described above

Table 5
Equilibrated Cell parameters of the orthorhombic simulation box, area per molecule, $\mathcal{A}$ and calculated density of the water/surfactant/Cn system for 1 to 12 molecules of 8-C16 surfactant at each interface

n_{surf}	a	b	c	A (Å^2)	Density (g/cm^3)
1	24.019	24.019	105.964	576.913	0.850
2	24.276	24.276	107.098	294.662	0.845
4	24.503	24.503	108.103	150.099	0.863
6	24.498	24.498	109.662	100.025	0.875
8	25.210	25.210	111.220	79.443	0.881
10	25.520	25.520	115.553	65.150	0.883
12	24.704	24.704	119.886	50.857	0.885

Table 6
Calculated *BE/area* for the water/8-C16/Cn interface, $n = 14$, 12, 11 and 10. For C14 the number of surfactant molecules, n_{surft}, is changed from 1 to 12

n_{surft}	-BE(Wat/C14)	-BE(Wat/8-C16)	-BE(C14/8-C16)
1	43.625	525.836	48.159
2	36.060	552.599	73.376
4	27.876	922.444	129.592
6	18.622	1184.124	152.920
8	9.368	1445.803	162.248
10	6.083	1422.520	147.674
12	2.797	1399.240	133.101
n_{surft}	-BE(Wat/C12)	-BE(Wat/8-C16)	-BE(C12/8-C16)
8	8.241	1482.277	150.016
n_{surft}	-BE(Wat/C11)	-BE(Wat/8-C16)	-BE(C11/8-C16)
8	9.048	1608.277	148.015
n_{surft}	BE(Wat/C10)	BE(Wat/8-C16)	-BE(C10/8-C16)
8	9.539	1203.351	142.445

were sequentially carried out to equilibrate the system. First, a NVT simulation was performed for 4 ns at 300K to thermalize and equilibrate the system. Then, a NPT simulation for 4ns was done to adjust the system to the right density. A final equilibration was performed by means of a NVT simulation for 4ns and the trajectories for these last NVT 2 ns were used for data analysis.

For C14, boxes with 1, 2, 4, 6, 8, 10 and 12 surfactant molecules in each interface were constructed. The resulting cell parameters of the simulation box, density and the area/molecule, $\mathcal{A}$ are collected in Table 5, while the *BE/area* between the different phase components are reported in Table 6. Comparison of A with *BE/area* and a polynomial regression have shown that the optimum value for the area/molecule corresponds to the case when there are eight surfactant molecules at the interface leading in this case to A = 79.44 Å^2. In agreement with experimental results [42] for mixtures of linear alkyl benzene sulfonate, for which sodium dodecyl benzene sulfonate is the primary component, the area/molecule at hydrocarbon/water interfaces in larger than the respective area at air/water interface. However, this value is only 5.44 units bigger to that obtained in the above section for the water/8-C16 interface, while the experimental reported valued at ref. [42] is significantly larger at the oil (soybean oil)/water interface (106 Å^2) than the air/water interface (83 Å^2). This last value is significantly bigger than the reported experimental range (43 to 65 Å^2) [41] for pure dodecyl benzene sulfonate.

For this surfactant molecule coverage, Fig. 5(b) shows the density profile along the z-axis direction. The original *IT* of 4.83 Å for the water/C14 interface increases to 18.77 Å. In this case, due to the presence of surfactant molecules, the interfacial thickness consists of three components: *IT* of the water interface, *IT* of the surfactant and *IT* of the C14 interface. Interestingly, the broadening of the interface

mainly occurs in the hydrocarbon side. Note that the sulfonate and benzene ring are mainly inside the water interface while the nonpolar tail groups tend to avoid the water molecules. Note (see Fig. 5a) that when the 8-C16 molecules substitute water and C14 molecules at the original water/C14 interface, the interaction across the interface occurs between the surfactant hydrophilic head and water molecules on one side of the interface and between the alkyl tail and C14 molecules on the other side of the interface. It is well known [29] that these interactions have to be much stronger than the original ones between immiscible phases such as C14 and water. Our results (see Table 6) suggest that the *BE/area* of the 8-C16/C14 and the water/8-C16 interfaces are about 3 and 29 times larger, respectively, than that of the water/C14 (49.10 dyn/cm) interface. It is clear that the hydrophilic groups provide very strong interactions between the surfactant molecules adsorbed at the water interface and the molecules of the solvent. These results are coherent with reported values for the free energies of solvation, ΔG_S, of alkanes in water [43], alkanes in alkanes [44] and ionic molecules in water [45]. For example, for octane in water and octane in decane the values of ΔG_S are 12.09 and -21.92 KJ/mol, respectively, while the reported solvation free energy for 90 anions [44] ranges from -57.80 for $[NO_2\text{-}C_6H_4\text{-}O]^-$ to -437.48 KJ/mol for $[HO]^-$. As one would expect, the interactions between phases formed by polar and ionic molecules are much more favorable than the interactions between phases where dispersive forces are the main ones. This is the origin of the surfactant effect: it changes unfavorable interactions between molecules having different natures (polar/non polar) by allowing the generation of very favorable interactions at the interface between molecules with similar character (polar/ionic or non-polar/non-polar).

Finally we have studied the effect of the alkane scanning on the calculated *BE/area* parameter for the 8-C16 surfactant, water interfaces with C10, C11 and C12 hydrocarbons were additionally studied and the results are also collected in Table 6. It is well known [11] that n_{min} in alkane interfacial tension scanning curve can represent the hydrophilic-lipophilic ability of surfactant, the lower the n_{min} value is, the more hydrophilic the surfactant is. Reduction of IFT depends directly on the replacement of solvent at the interface by molecules of surfactant. The tension across the interface is significantly reduced by the adsorption of surfactant molecules because these interactions are much stronger than the original interaction between the hydrocarbon and water molecules. In general, the higher the interfacial surfactant concentration is, the lower the IFT is. From Table 6 it can be seen that the *BE/area* absolute value of the water-head of 8C16 shows a maximum just at C11. The obtained trend for this interaction is C10 (1203.351 dyn/cm) $<$ C11 (1608.277 dyn/cm) $>$ C12 (1482.277 dyn/cm) $>$ C14 (1445.803) while for the tail-alkane interaction the *BE/area* systematically increases as the chain length of Cn increases, C10 (142.44) $<$ C11 (148.015) $<$ C12 (150.02) $<$ C14 (162.25). This result shows that for the water/8-C16/Cn interface it is this trend in adhesion of the surfactant in the water phase that defines the n_{min} value of *IFT* and not the interaction between surfactant molecules. In this manner we are able to rationalize the observed facts by resorting to the concept of binding energy per area as a measured of the adhesion forces.

4. Conclusions

This work reports on a systematic study using molecular dynamics simulations of the density profiles and the adhesion forces (binding energy per cross sectional area, *BE/area*) for the water/n-alkane (hexane, octane, decane, dodecane and tetradecane) interfaces. The calculated interfacial thickness, *IT*, and BE/area are in good agreement with reported experimental values and both of these quantities grow monotonically with the atom carbon number. Excellent linear correlations with the carbon number were

obtained ($IT_{calc} = 0.136\ n_{Ci} + 2.964$; $R^2 = 0.99$). Values of *BE/area* ranging from 46.69 for C6 to 49.10 for C14 were calculated.

Similar studies for the vacuum/sodium O-(1-heptylnonyl) benzene sulfonate (8-C16)/water interface were carried out. The optimum minimal area per molecule at the interface, $\mathcal{A}$, the *BE/area* and profiles densities were determined. These are: A =74.0 Å^2, IT = 6.7 Å and *BE/area* = 1502.462 dyn/cm. This study shows the presence of strong interactions between the surfactant polar head group with sodium and water molecules. The density profile suggests that the surfactant head ($NaSO_3$-benzene) is almost entirely hydrated and that it is located in the inside the interface while the carbon tails are almost excluded from the water/8-C16 interface.

The effect of 8-C16 on the interfaces n-hydrocarbon/ 8-C16/water were also explored. For C14, an optimum value of around eight surfactant molecules forming the monolayer at the interface was found; this corresponds to a value of $A = 79.44$ Å^2. The calculated *BE/area* values of -162.25 and -1445.80 dyn/cm for the 8-C14/C14 and water/8-C14 interface sides, respectively, were found. It is clear that the hydrophilic surfactant-head provides very strong adhesive interaction and miscibility with the water phase. Scanning of BE/area against Cn (C10, C11, C12 and C14) have shown that the magnitude of the binding per area of the tail-Cn interaction at the interface systematically increases as the chain length of Cn increases, whereas, in agreement with the experimental *IFT* values, the *BE/area* at the interface for the water-head interaction shows a maximum at C11. These results suggest that for the water/8-C16/Cn interface, the n_{min} of *IFT* is mainly determined by the trends of adhesion of the surfactant head with the water molecules at the interface.

Acknowledgements

Y.A. and R. P would like to thank SENESCYT (Secretaría Nacional de Educación Superior, Ciencia, Tecnologiía e Innovacioón) for giving them the opportunity to participate in the Prometheus Program. Y. A gratefully acknowledges the National Council of Science and Technology of Mexico (CONACYT) for financial support during 2010 through sabbatical year grant 0129145 at Instituto de Matematicas, Unidad Cuernavaca

References

[1] H-Q. Sun, H-Y. Xiao and X-H. Liu, *Sci. China Chem* **54** (2011), 1078–1085.
[2] Y-P. Huang, L. Zhang, L. Zhang, L. Luo, S. Zhao and J-Y. Yu, *J. Phys. Chem. B* **111** (2007), 5640–5647.
[3] X-W. Song, L. Wang, Z-Q. Li, L. Luo, L. Zhang, S. Zhao and J-Y. Yu, *J. Disp. Sci. Tech.* **28** (2007), 825–828.
[4] (a) P.H. Doe, W.H. Wade and R.S. Schechter, *J. Colloid Interface Sci.* **59** (1977), 525–531. (b) P.H. Doe, M. El-Mary and W.H. Wade, *J. Am. Oil Chem. Soc.* **54** (1977), 570–577.
[5] L. Peltonen, J. Hirvonen and J. Yliruusi, *J. Colloid Interface Sci.* **240** (2001), 272–276.
[6] M.D. Urzua, F.J. Mendizabal, W.J. Cabrera and H.E. Rios, *J. Colloid Interface Sci.* **281** (2005), 93–100.
[7] M. Pisarcik, M.J. Rosen, M. Polakovicova, F. Devinsky and I. Lacko, *J. Colloid Interface Sci.* **289** (2005), 560–565.
[8] J. Yang, W. Qiao, Z. Li and L. Cheng, *Fuel* **84** 2005), 1607–1611.
[9] Z. Zhao, F. Liu, W. Qiao, Z. Li and L. Cheng, *Fuel* **85** (2006), 1815–1820.
[10] K.D. Danov and P.A. Kralchesky, *Colloid J* **74** (2012), 172–185.
[11] L.-C.H. Wang, S.-J. Liu, J.-C.H. Zhang, Z.-Q. Li, L. Wang and S.-X. Jiang, *J. Disp. Sci. Tech.*, in press, (2013). DOI: 10.1080/01932691.2013.769108.
[12] R. Varadaraj, J. Bock, S. Zusma and N. Brons, *Langmuir* **8** (1992), 14–17.
[13] K. Chari, Y.-S. Seo and S. Satija, *J. Phys. Chem. B.* **108** (2004), 11442–11446.
[14] G.-M. Qu, W. Ding, T. Yu and J.-Ch. Cheng, *J. Surfact. Deterg.* **13** (2010), 149–153.
[15] G.B. Ray, I. Chakraborty, S. Ghosh and S.P. Moulik, *Colloid Polym. Sci.* **285** (2007), 457–469.

[16] H. Nakahara, O. Shibata and Y. Moroi, *J. Phys. Chem. B.* **115** (2011), 9077–9086.
[17] J. Bocker, M. Schlemkrick, P. Bopp and J. Brickmann, *J. Phys. Chem.* **96** (1992), 9915–9922.
[18] M. Tarek, D.J. Tobias and M.L. Klein, *J. Phys. Chem.* **99** (1995), 1393–1402.
[19] S. Yuan, L. Ma, X. Zhang and L. Zheng, *Colloids Surf. A: Phys. Eng. Aspects* **289** (2006), 1–9.
[20] X. He, O. Guvench, A.D. MacKerell and M.L. Klein, *J. Phys. Chem. B.* **114** (2010), 9787–9794.
[21] T. Zhao, G. Xu, S. Yuan, Y. Chen and H. Yan, *J. Phys. Chem. B.* **114** (2010), 5025–5033.
[22] J. Pang, Y. Wang, G. Xu and T. Han, *J. Phys. Chem. B.* **115** (2011), 2518–2526.
[23] S.S. Jang, S.-T. Lin, P.K. Maiti, M. Blanco and W.A. Goddard, III., *J. Phys. Chem. B.* **108** (2004), 12130–12140.
[24] (a) H.-Y. Xiao, Z. Zhen, H.-Q. Sun, X.-L. Cao, Z.-Q. Li, X.-W. Song, X.-H. Cui and X.-H. Liu, *Acta Phys. Chim. Sin.* **26** (2010), 422–428. (b) C.D. Wick, T.-M.C. Hang, J.A. Slocum andO.T. Cummings. *J. Phys. Chem. C.* **116** (2012), 783.
[25] J.N. Israelachvili, *Intermolecular and Surfaces Forces*, Second Edition, Academic Press, Elsevier, 2006.
[26] W.R. Gillap, N.D. Weiner and M. Gibaldi, *J. Am. Oil Chem. Soc.* **44** (1967), 71–73.
[27] S. Zeppieri, J. Rodriguez and A.L. Lopez de Ramos, *J. Chem. Data* **46** (2001), 1086–1088.
[28] A. Goebel and K. Lunkenheimer, *Langmuir* **13** (1997), 369–372.
[29] M.J. Rosen, *Surfactants and Interfacial Phenomena*, Third Edition, John Wiley & sons, 2004.
[30] Amorphous Cell is available as part of Material Studio. Accelrys Inc. San Diego. USA. 2012.
[31] Forcite is available as part of Material Studio. Accelrys Inc. San Diego. USA. 2012.
[32] (a) H. Sun, *J. Phys. Chem. B.* **102** (1998), 7338. (b) B.E. Eichinger, D. Rigby and J. Stein, *Polymer* **43** (2002), 599. (c) B.E. Eichinger, D. Rigby and M.H. Muir, *Comp. Polym. Sci.* **5** (1995), 147.
[33] R. Aveyard and D.A. Haydon, *Trans. Faraday Soc.* **61** (1965), 2255.
[34] D.M. Mitrinovic, A.M. Tikhonov, M. Li, Z. Huang and M.L. Schlossman, *Phys. Rev. Lett.* **85** (2000), 582.
[35] J.C. Conboy, J.L. Daschbach and G.L. Richmond, *Appl. Phys. A* **59** (1994), 623–629.
[36] J.L. Rivera, C. McCabem and P.T. Cummings, *Phys. Rev. E.* **67** (2003), 011603.
[37] A.J. Riedleder, S.E. Kentish, J.M. Perere and G.W. Stevens, *Solvent Extract. and Ion Exchan* **25** (2007), 41–52.
[38] H.Y. Xiao, Z. Zhen, H.Q. Sun, X.L. Cao, Z.Q. Li, X.W. Song, X.H. Cui and X.H. Liu, *Sci. Ch. Chem* **53** (2010), 945–949.
[39] H. Lavoie, B. Desbat, D. Vaknin and C. Salesse, *Biochemistry* **41** (2002), 13424.
[40] Q. He, X. Zhai and J. Li, *J. Phys. Chem B* **108** (2004), 473.
[41] J.-G. Ma, B.J. Boyd and C.J. Drummond, *Langmuir* **22** (2006), 8046.
[42] S.E. Anachkov, S. Tcholakova, D.T. Dimitrova, N.D. Denkov, N. Subrahmaniam and P. Bhunia, *Colloid Surf. A: Phys. Eng. Aspects* **466** (2015), 18.
[43] N.M. Garrido, A.J. Queimada, M. Jorge, E.A. Macedo and I.G. Economou, *J. Chem. Theo. Comp.* **5** (2009), 2436.
[44] D.J. Giesen, Ch.J. Cramer and D.G. Truhlar, *J. Phys. Chem* **99** (1995), 7137.
[45] S. Lee, K.-H. Cho, Ch.J. Lee, G.E. Kim, Ch.H. Na, Y. In and K.T. No, *J. Chem. Inf. Model.* **5**(51) (2011), 105.
[46] S.C. Ayirala and D.N. Rao, *Fluid Pha. Equil.* **249** (2006), 82.